International Journal of Mathematical, Engineering and Management Sciences
Vol. 10, No. 2, 420-440, 2025
https://doi.org/10.33889/IJMEMS.2025.10.2.021

Ram Arti Publishers

Optimal Covid-19 Control on Effectiveness of Detection Campaign and Treatment

Mouhamadou A. M. T. Baldé
Laboratory of Mathematics of Decision and Numerical Analysis,
University of Cheikh Anta Diop, BP, 5005, Dakar, Senegal.
E-mail: mouhamadoualioumountagatall.balde@ucad.edu.sn

Sidy Ly
Laboratory of Mathematics of Decision and Numerical Analysis,
University of Cheikh Anta Diop, BP, 5005, Dakar, Senegal.
Corresponding author: sidy1.ly@ucad.edu.sn

Léna Tendeng
Laboratory of Mathematics of Decision and Numerical Analysis,
University of Cheikh Anta Diop, BP, 5005, Dakar, Senegal.
E-mail: ndeyelena.tendeng@ucad.edu.sn

(Received on June 11, 2024; Revised on September 8, 2024 & December 8, 2024; Accepted on January 10, 2025)

Abstract
The COVID-19 pandemic has seen the development of several mathematical models. In recent years, the very topical issue of re-susceptibility has led to the proposal of more complex models to address this issue. The paper deals with an optimal control problem applied to COVID-19. The Pontryagin maximum principle and the dynamic programming principle are used to solve the problem. A compartmental Ordinary Differential Equation (ODE) model is proposed to study the evolution of the pandemic by controlling the effectiveness of the detection campaign and the treatment. We prove the global stability of the Disease-Free Equilibrium (DFE) and the existence of optimal control and trajectories of the model. In the optimal control problem, we bring the system back to the DFE. Numerical simulations based on COVID-19 data in Senegal show possibilities to reduce the disease evolution, sometimes by emphasizing the detection campaign and/or the treatment proposed to patients.

Keywords- Differential equations, Dynamic programming principle, Hamilton-Jacobi-Bellman equations, Pontryagin maximum principle, Covid-19.

1. Introduction

The COVID-19 pandemic began on November 16, 2019, in Wuhan, Hubei Province (in central China). Subsequently, it spread worldwide and was officially declared a pandemic by the World Health Organization (WHO) on March 11, 2020. Some countries have taken emergency measures such as social distancing, confinements, etc. Subsequently, vaccines were developed, and vaccination campaigns were carried out. On May 5, 2023, the WHO declared the end of the international health emergency (Wikipedia). However, in some countries, COVID-19 is not yet under control. It is always interesting to study strategies to control the disease.

Many methods have been used to study the evolution of the COVID-19 pandemic. Many authors (Balde, 2020; Balde et al., 2020; Ndiaye et al., 2020a; Ndiaye et al., 2020b) have used machine learning to analyze and predict the evolution of the pandemic. Neural networks are widely used. Other authors use stochastic models to study the Covid-19 pandemic (Ly et al., 2022). Research into stochastic and deterministic optimal control is also carried out in the analysis to implement strategies to limit the evolution of the pandemic

(Firmansyah and Rangkuti, 2023; Kifle and Obsu, 2023; Ly et al., 2022; Mansal et al., 2024). In Wang et al. (2022), authors have used an integral-differential equation model involving the vaccination effect and the incubation of COVID-19. The authors in the paper (Ahmed et al., 2021) proposed a mathematical model using the Ordinary Differential Equation (ODE) and Fractional Differential Equation. In Firmansyah and Rangkuti (2023), the authors performed a sensitivity analysis using a sensitivity index to measure the relative change in the basic reproduction number for each parameter, and this control function was applied to the dynamic modeling of the spread of COVID-19 using the Pontryagin Minimum Principle. Kifle and Obsu (2023) show that simultaneously reducing potential contact between susceptible and infected individuals, implementing effective contact tracing and quarantine, isolation of symptomatically infected individuals, and providing effective treatment are the optimal mechanisms to halt the spread of COVID-19 disease in the community. In Ng and Gui (2020), the authors studied an ordinary differential equation model including a time delay at which the immunity of individuals previously healed ends.

Some people can contract the disease a second time after an initial recovery. This fact has motivated the development and study of models that consider cases of re-susceptibility (Ng and Gui, 2020; Ly et al., 2022).

Likewise, current COVID-19 vaccines are not guaranteed at 100%. That is why people take multiple vaccination doses at specific times, raising the question of re-susceptibility. In Ng and Gui (2020), authors show that re-susceptibility may lead to subsequent waves of infections in the future depending on the time of temporal immunity. In Firmansyah and Rangkuti (2023), by using three types of control acting on awareness, personal defenses, and the care of patients and vaccinating a proportion of the population, the transmission can be overcome in a few days. In Mansal et al. (2024), the authors analyze two optimal control strategies to reduce the spread of COVID-19. The authors use three controls acting on distancing, case detection and effort of cure like financial support. They show that increasing educational campaigns, disease tests, and financial support to ensure drugs for infected individuals can reduce the number of infected and dead.

We propose a compartmental model studied in a previous stochastic optimal control paper (Ly et al., 2022). The model takes vaccination and re-susceptibility into account. Deterministic optimal control theory is used to analyze strategies to reduce the evolution of COVID-19. Managing the proportion of vaccinated and controlling the detection and treatment of patients can prevent subsequent waves of infection.

The disease-free equilibrium (DFE), which is globally asymptotically stable, is calculated and used in the objective function of the optimal control problem to bring the optimal states closer to this equilibrium.

Considering re-susceptibility in the model is a significant contribution to this paper. Likewise, mathematical contributions are to be emphasized. Proving a result of global stability can be challenging. The use of dynamic programming to solve optimal control problems should be noted because the Pontryagin maximum principle is applied in most articles on control.

The paper is structured as follows: In Section 2, we propose a compartmental model of COVID-19 composed of susceptible, exposed, detected, and undetected infected, hospitalized, and recovered. In Section 3, a mathematical analysis of the model is performed by calculating the basic reproduction number and proving the DFE's global stability. We demonstrate the existence of control and optimal states of the optimal control problem, which is solved by the Pontryagin Maximum Principle (PMP) and Dynamic Programming Principle (DPP) in Section 4. Section 5 illustrates and discusses the theoretical results obtained by numerical simulations based on COVID-19 data in Senegal. A conclusion is done in Section 6.

2. Modeling

A compartmental diagram **Figure 1**, from a previous paper (Ly et al., 2022), is recalled from which is derived the model. This model is composed of six compartments $S(t)$, $E(t)$, $U(t)$, $V(t)$, $H(t)$ and $R(t)$ respectively designating susceptible, exposed, undetected infected, confirmed infected, hospitalized and immunized at time t. The compartment R represents immunized by vaccination (coming from S) and recovered (coming from H and U).

The major hypotheses of the model are:

- Natural mortalities are not considered. In a small-time interval, natural mortality is negligible compared to that caused by disease.
- Newborns are not susceptible to contracting the disease. WHO data for Senegal have not recorded a significant case of newborns contracting COVID-19.
- Only a portion of susceptible people are vaccinated. Indeed, the vaccine is not compulsory in certain countries, such as Senegal, and often arouses fear in certain individuals.
- R individuals are not totally immunized. Immunity acquired after recovery or after vaccination is not total, which is why a proportion δ of the R individuals become susceptible again, hence the question of re-susceptibility (Ly et al., 2022; Ng and Gui, 2020).

The ODE corresponding to the model is given as follows:

$$\begin{cases} \dot{S}(t) = \delta R - \beta_u SU - \beta_v SV - \eta S \\ \dot{E}(t) = \beta_u SU + \beta_v SV - \nu_1 E - \nu_2 E \\ \dot{U}(t) = \nu_1 E - d_1 U - \xi U \\ \dot{V}(t) = \nu_2 E - \alpha V - d_2 V \\ \dot{H}(t) = \alpha V - d_3 H - \gamma H \\ \dot{R}(t) = \xi U + \gamma H + \eta S - \delta R \end{cases} \quad (1)$$

under initial conditions:

$$\begin{cases} S(0) = S_0, \quad E(0) = E_0, \quad U(0) = U_0, \\ V(0) = V_0, \quad H(0) = H_0, \quad R(0) = R_0 \end{cases} \quad (2)$$

The coefficients used to switch from one compartment to another and the meaning of each compartment are described in **Table 1**.

Table 1. Variables and parameters used in the model.

Variables and parameters	Descriptions
β_u	transmission rate of undetected
β_v	transmission rate of confirmed
ν_1	Rate of incubation or latency of undetected
ν_2	rate of incubation or latency of confirmed
d_1	death rate of undetected
d_2	death rate of confirmed
d_3	death rate of hospitalized patient
α	rate of hospitalized from confirmed
γ	rate of hospitalized patients becoming recover
δ	rate of recovered becoming susceptible again
η	vaccination rate
ξ	rate of recovered from undetected
$S(t)$	Number of individuals susceptible to contracting the disease at time t
$E(t)$	Number of individuals exposed to the disease at time t

Table 1 continued…

$U(t)$	Number of unknown infected at time t
$V(t)$	Number of known infected at time t
$H(t)$	Number of infected individuals hospitalized at time t
$R(t)$	Number of individuals recovered from the disease at time t
$N(t)$	Total population at time t, $N(t) = S(t) + E(t) + U(t) + V(t) + H(t) + R(t)$
N_0	Initial population $N_0 = N(0)$

The graph (**Figure 1**) summarizes concisely the model.

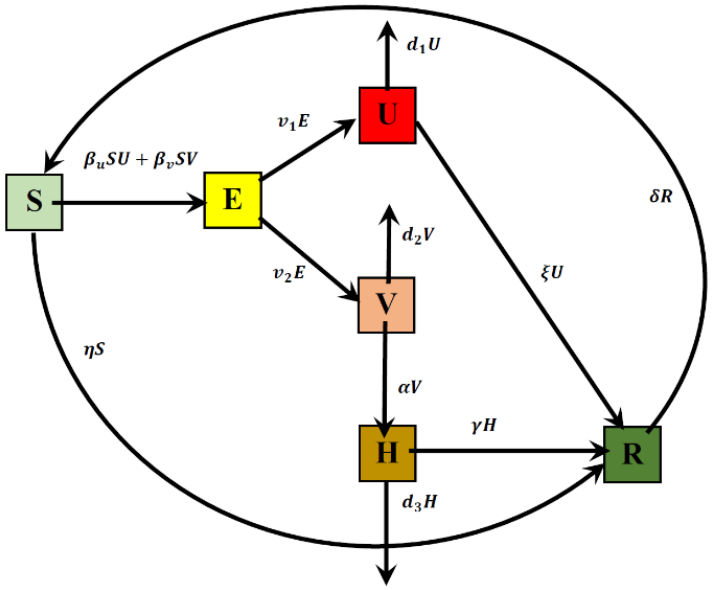

Figure 1. Compartmental diagram of COVID-19.

3. Mathematical Analysis

In this section, we perform a mathematical analysis of the model (1) that is we study the well-posedness of the system, we calculate the Disease-Free Equilibrium (DFE) and the basic reproduction number. Finally, we prove the global stability of the DFE.

3.1 Well-Posedness of the Model

Let's set the domain

$\mathcal{D} = \{(\mathrm{S(t), E(t), U(t), V(t), H(t), R(t)}) \in \mathbb{R}_+^6 : 0 \leq \mathrm{N(t)} \leq \mathrm{N}_0\}$.

Theorem 1. $\mathcal{D}$ is positively invariant for the flow of the system (1).

***Proof*:** Consider any time $t > 0$ and for all time $0 \leq r < t$, we have $S(r) > 0, \quad E(r) > 0, \quad U(r) > 0, \quad V(r) > 0, \quad H(r) > 0, \quad R(r) > 0$.

Consider the first equation of the system (1) $\dot{S}(t) = \delta R - \beta_u SU - \beta_v SV - \eta S$. It can be rewritten in following form $\dot{S}(t) = \delta R(t) - (\xi + \eta)S$.

Now, using the Duhamel formula (Teschl, 2012):

$$S(t) = S_0 \exp\left(-\int_0^t (\xi(s)+\eta)ds\right) + \int_0^t \left[\delta R(\tau) \exp\left(-\int_\tau^t (\xi(s)+\eta)ds\right)\right] d\tau$$

$$S(t) = S_0 \exp\left(-\eta t - \int_0^t \xi(s)ds\right) + \exp\left(-\eta t - \int_0^t \xi(s)ds\right) \int_0^t \left[\delta R(\tau) \exp\left(\int_0^\tau (\xi(s)+\eta)ds\right)\right] d\tau$$

$$S(t) = \exp\left(-\eta t - \int_0^t \xi(s)ds\right)\left[S_0 + \int_0^t \left(\delta R(\tau) \exp\left(\eta\tau + \int_0^\tau \xi(s)ds\right)\right) d\tau\right].$$

Finally, since $S_0 > 0$, for any $\tau < t$, $R(\tau) > 0$, we obtain $S(t) > 0$.

Similar work for $E,\ U,\ V,\ H,\ R$ gives $E(t) > 0$, $U(t) > 0$, $V(t) > 0$, $H(t) > 0$, $R(t) > 0$ for all time. $t > 0$.

It remains to prove that $\mathcal{D}$ is bounded. Summing all equations of the system (1), yields $\frac{dN}{dt} = -d_1 U - d_2 V - d_3 H \leq 0$.

Now, integrating gives $\int_0^t \frac{dN}{dt} ds \leq 0$. Then, $N(t) - N_0 \leq 0$. And finally, $N(t) \leq N_0$.

3.2 Basic Reproduction Number $\mathcal{R}_0$

The Disease-Free Equilibrium (DFE) of the model (1) is determined by setting $E = U = V = H = \dot{S} = \dot{E} = \dot{U} = \dot{V} = \dot{H} = \dot{R} = 0$ in the system (1). We obtain $\eta S - \delta R = 0$, then $R = \frac{\delta}{\eta} S$.

$S + R \leq N_0$ gives $S \leq \frac{\delta}{\delta+\eta} N_0$.

Finally, the DFE of the model (1) is $X^* = (S^*, 0,0,0,0, R^*)$ with $S^* = \frac{\delta}{\delta+\eta} N_0$ and $R^* = \frac{\eta}{\delta+\eta} N_0$.

Following the work in (Van den Driessche and Watmough, 2002), we consider the infected compartments $(E,\ U,\ V,\ H)$. Applying the lemma 1 (p. 32) in Van den Driessche and Watmough (2002), the gradient at the DFE is

$$\boldsymbol{J} = \nabla_{(E,U,V,H)} \begin{pmatrix} \beta_u SU + \beta_v SV - \nu_1 E - \nu_2 E \\ \nu_1 E - d_1 U - \xi U \\ \nu_2 E - \alpha V - d_2 V \\ \alpha V - d_3 H - \gamma H \end{pmatrix}_{|X^*}$$

$$\boldsymbol{J} = \begin{pmatrix} -\nu_1 - \nu_2 & \frac{N_0 \beta_u \delta}{\delta+\eta} & \frac{N_0 \beta_v \delta}{\delta+\eta} & 0 \\ \nu_1 & -d_1 - \xi & 0 & 0 \\ \nu_2 & 0 & -\alpha - d_2 & 0 \\ 0 & 0 & \alpha & -d_3 - \gamma \end{pmatrix}$$

$J = F - V$, with

$$F = \begin{pmatrix} 0 & \frac{N_0\beta_u\delta}{\delta+\eta} & \frac{N_0\beta_v\delta}{\delta+\eta} & 0 \\ \nu_1 & 0 & 0 & 0 \\ \nu_2 & 0 & 0 & 0 \\ 0 & 0 & \alpha & 0 \end{pmatrix}, V = \begin{pmatrix} \nu_1+\nu_2 & 0 & 0 & 0 \\ 0 & d_3+\gamma & 0 & 0 \\ 0 & 0 & d_1+\xi & 0 \\ 0 & 0 & 0 & \alpha+d_2 \end{pmatrix}.$$

F is non-negative and V is nonsingular. Finally, we get,

$$\mathcal{R}_0 = \rho(FV^{-1})$$

$$\mathcal{R}_0 = \sqrt{\frac{N_0\delta(\alpha\beta_u\nu_1+\beta_u d_2\nu_1+\beta_v d_1\nu_2+\beta_v\nu_2\xi)}{(\alpha+d_2)(d_1+\xi)(\delta+\eta)(\nu_1+\nu_2)}}$$

$$\mathcal{R}_0 = \sqrt{N_0\delta\frac{\beta_u\nu_1(\alpha+d_2)+\beta_v\nu_2(d_1+\xi)}{(\alpha+d_2)(d_1+\xi)(\delta+\eta)(\nu_1+\nu_2)}}.$$

3.3 Global Stability of the DFE

This subsection shows that the DFE is globally asymptotically stable as soon as $\mathcal{R}_0$ satisfies a specific condition.

Theorem 2. *The disease-free equilibrium of the system* (1) *is globally asymptotically stable in* $\overline{\mathcal{D}}$ *if and only if* $\mathcal{R}_0 \leq 1$.

***Proof*:** For this aim we use Theorem 4.5 (p. 6) and its corollary in the paper Kamgang and Sallet (2008).

We consider the following splitting of states variables (x_1, x_2), where $x_1 = (S, R)$ and $x_2 = (H, E, U, V)$corresponds to infected compartment.

As proved above, the domain $\mathcal{D}$ is positively invariant. Hence, the hypothesis $\mathbf{H}_1$ is satisfied.

In the model (1), the sub-system $\dot{x}_1 = \mathbf{A}_1(x_1, 0)(x_1 - x_1^*)$ is such that: $x_1^* = (S^*, R^*)$ corresponds to the DFE and

$$\mathbf{A}_1(x_1, 0) = \begin{pmatrix} -\eta & \delta \\ \eta & -\delta \end{pmatrix}.$$

The two eigenvalues of this sub-matrix are 0 and $-(\eta+\delta)$. To obtain asymptotic stability of the DFE in $\mathcal{D}$, we consider the fact that without disease $S + R = N_0$ since $\dot{S} + \dot{R} = 0$. That implies $R = N_0 - S$ and replacing that in the first equation of the sub-system gives $\dot{S} = -(\eta+\delta)S + \delta N_0$. Hence, $S(t) = S_0\exp(-(\eta+\delta)t) + \frac{\delta}{\eta+\delta}N_0$. We see that $\lim_{t\to+\infty} S(t) = \frac{\delta}{\eta+\delta}N_0 = S^*$.

Finally, this sub-system is globally asymptotically stable at the DFE. Then the hypothesis $\mathbf{H}_2$ is satisfied. The sub-matrix $A_2(x)$ is given by:

$$\begin{pmatrix} -d_3-\gamma & 0 & 0 & \alpha \\ 0 & -\nu_1-\nu_2 & \beta_u S & \beta_v S \\ 0 & \nu_1 & -d_1-\xi & 0 \\ 0 & \nu_2 & 0 & -\alpha-d_2 \end{pmatrix}.$$

Now we are going to verify the hypothesis $\mathbf{H}_3', \mathbf{H}_4', \mathbf{H}_5'$. We write the matrix in the following block form:

$$\begin{pmatrix} \mathbf{A}_2^{1,1} & \mathbf{A}_2^{1,2} \\ 0 & \mathbf{A}_2^{2,2} \end{pmatrix}$$

where, $\mathbf{A}_2^{1,1} = -d_3 - \gamma$, $\mathbf{A}_2^{1,2} = (0,0,\alpha)$,

$$\mathbf{A}_2^{2,2} = \begin{pmatrix} -\nu_1 - \nu_2 & \beta_u S & \beta_v S \\ \nu_1 & -d_1 - \xi & 0 \\ \nu_2 & 0 & -\alpha - d_2 \end{pmatrix}.$$

$\mathbf{A}_2^{1,1}$ and $\mathbf{A}_2^{2,2}$ are both irreducible. Hence, $\mathbf{H}_3'$ is satisfied.
$\mathbf{A}_2^{1,1}$ and $\mathbf{A}_2^{2,2}$ are both bounded at the DFE in $\mathcal{D}$. Indeed, by denoting $\overleftarrow{\mathbf{A}}_2^{1,1}$ and $\overleftarrow{\mathbf{A}}_2^{2,2}$ their respective bound, we have $\mathbf{A}_2^{1,1}$ is constant then $\overleftarrow{\mathbf{A}}_2^{1,1} = \mathbf{A}_2^{1,1}$ and

$$\overleftarrow{\mathbf{A}}_2^{2,2} = \begin{pmatrix} -\nu_1 - \nu_2 & \frac{N_0\beta_u\delta}{\delta+\eta} & \frac{N_0\beta_v\delta}{\delta+\eta} \\ \nu_1 & -d_1 - \xi & 0 \\ \nu_2 & 0 & -\alpha - d_2 \end{pmatrix}.$$

The hypothesis $\mathbf{H}_5'$ is equivalent to $\mathcal{R}_0 \leq 1$ see Kamgang and Sallet (2008).

4. Optimal Control Problem (OCP)

The objective of the section is to solve a deterministic optimal control problem. The idea is to act on the system (1) by keeping it around the DFE through the detection campaign and treatment offered to hospitalized patients defined respectively by the parameters $a_1(t)$ and $a_2(t)$ which are the components of the control vector $a \in \mathcal{A} = \{a: [0;T] \to [0;1]^2, \text{measurable}\}$ with $(0 \leq a_i(t) \leq 1$ for $i = 1;2)$. Thus, the variables ν_2 and γ can be respectively replaced by $a_1\nu_2$ and $a_2\gamma$. The system (1) is then rewritten as follows:

$$\begin{cases} \dot{S}(t) = \delta R - \beta_u SU - \beta_v SV - \eta S \\ \dot{E}(t) = \beta_u SU + \beta_v SV - \nu_1 E - a_1\nu_2 E \\ \dot{U}(t) = \nu_1 E - d_1 U - \xi U \\ \dot{V}(t) = a_1\nu_2 E - \alpha V - d_2 V \\ \dot{H}(t) = \alpha V - d_3 H - a_2\gamma H \\ \dot{R}(t) = \xi U + a_2\gamma H + \eta S - \delta R \end{cases} \tag{4}$$

The objective function is then defined by:

$$J(a) \quad = \quad \frac{1}{2}\int_0^T ((S - S^*)^2 + E^2 + U^2 + V^2 + H^2 + (R - R^*)^2 + \varepsilon_1 a_1^2 + \varepsilon_2 a_2^2)\, dt \tag{5}$$

with $\epsilon_1, \epsilon_2 > 0$.

Let's set the integrand

$$L(t,\mathrm{X}, a) = \quad \frac{1}{2}((S - S^*)^2 + E^2 + U^2 + V^2 + H^2 + (R - R^*)^2 + \varepsilon_1 a_1^2 + \varepsilon_2 a_2^2)$$

$$L(t,\mathrm{X}, a) = (\| \boldsymbol{X}(t) - \boldsymbol{X}^*(t) \|^2 + \varepsilon_1 a_1^2 + \varepsilon_2 a_2^2) \tag{6}$$

Optimal control problem is defined as follow: Find $a^* = (a_1^*, a_1^*)$ such that

$$J(a^*) = \min_{a \in \mathcal{A}} J(a) \tag{7}$$

on the set $\mathcal{A} = \{a: [0;T] \to [0;1]^2$, measurable$\}$ under the constraints of Equation (1).

Let's denote
$\mathcal{F} = \{(\boldsymbol{X}, a)$ feasible for $(7)\}$,
the set of feasible pair (X, a).

4.1 Trajectories Analysis

Let $f = (f_i)_{i\in\Lambda}$ be the right-hand side of Equation (1) for $X_i -$ compartment where $i \in \Lambda = \{1, \dots, 6\}$. Let's recall $\mathcal{D}$ defined as in Section 3.1 and N_0 the initial total size of the population. The system (4) can be rewritten as follows:

$$\dot{\mathbf{X}}_i = f_i(\mathbf{X}, a) \text{ for } i \in \Lambda \tag{8}$$

with X_i is the $i -$th component of the vector state $\mathbf{X} = (S, E, U, V, H, R)^T$ of the system and a the control. We see that the function $f \in \mathcal{C}^1(\mathcal{D} \times [0;1]^2; \mathbb{R}^6)$.

The following theorem ensures the existence of a unique solution.

Theorem 3. *For any control* $\mathrm{a}(\cdot) \in [0;1]^2$, *the system* (4) *has a unique, Lipschitz continuous solution.*

***Proof*:** Following Fleming et al. (1975) it suffices to show that for all $\mathbf{X} = (S, E, U, V, H, R)^T$ and $\mathbf{Y} = (S', E', U', V', H', R')^T$ in $\mathcal{D}$ and $\mathrm{a}(\cdot) \in [0;1]^2$, there exists a constant C such that:

$$\begin{cases} \| f(\mathbf{X}, a) \| \leq C \\ \| f(\mathbf{X}, a) - f(\mathbf{Y}, a) \| \leq C \| \mathbf{X} - \mathbf{Y} \| \end{cases} \tag{9}$$

Since f is at least C^1 with respect to its variables $t, \mathbf{X}, a$ in bounded set $\mathcal{D} \times [0;1]^2; \mathbb{R}^6$ the condition (9) is immediately satisfied.

We now discuss the existence of an optimal control pair a^* by proving that under certain conditions the following theorem guarantees the existence of optimal control of the problems (7)-(4).

Theorem 4. *Consider the control problems* (7)-(4). *Since* (9) *is satisfied, there exists* $a^* \in \mathcal{A}$ *such that Equation* (7) *holds.*

***Proof*:** We use the existence theorem in Fleming et al. (1975) theorem III. 4.1. p.68-69. Since Equation (7) is satisfied, it remains to verify:

- $\mathcal{F}$ is not empty.
- $\mathcal{A}$ is convex and closed.
- The integrand of the objective functional is convex in $\mathcal{A}$.
- There exist constants $c_1, c_2 > 0$, and $\beta > 1$ such that the integrand $\mathrm{L}(t, X, a)$ of the objective functional satisfies.

$\mathrm{L}(t, X, a) \geq c_1(\| a \|^2)^{\beta/2} - c_2$.

The theorem 3 on the existence of solution of the system (4) ensures that $\mathcal{F}$ is not empty. Hence, condition 1 holds.
The set $[0;1]^2$ is convex and closed.
The integrand $L(t,\mathrm{X}, a)$ is convex.

For the fourth condition
$L(t,\mathrm{X}, a) = (\| \boldsymbol{X}(t) - \boldsymbol{X}^*(t) \|^2 + \varepsilon_1 a_1^2 + \varepsilon_2 a_2^2)$,

Since $\varepsilon_1, \varepsilon_2 > 0$, there exists $c_1 > 0$ with $\min(\varepsilon_1, \varepsilon_2) > c_1$such that $\varepsilon_1 a_1^2 + \varepsilon_2 a_2^2 \geq c_1 \parallel a(t) \parallel^2$.

Hence there exists $c_2 > 0$ such that $\varepsilon_1 a_1^2 + \varepsilon_2 a_2^2 \geq c_1 \parallel a(t) \parallel^2 - c_2$.

Finally, considering $\beta = 2$, the condition 4 holds.

We use Pontryagin's maximum principle to deal with the necessary optimality conditions and introduce the following Hamiltonian for optimal control problems (7)-(4):

$$\mathcal{H}(a) = \sum_{i\in\Lambda} p_i f_i + \frac{1}{2}((S - S^*)^2 + E^2 + U^2 + V^2 + H^2 + (R - R^*)^2 + \varepsilon_1 a_1^2 + \varepsilon_2 a_2^2) \quad (10)$$

where, $(p_i)_{i\in\Lambda}$ are adjoint functions and f_i is given by the right-hand side of Equation (4) for X_i −compartment.

Theorem 5. *Assuming a^* the optimal control of problems* (7)-(4) *and X^* the corresponding optimal trajectory. Then there exists an adjoint vector $(p_i)_{i\in\Lambda}$ such that the following systems hold:*

$$\begin{cases} \dot{S}(t) = \delta R - \beta_u SU - \beta_v SV - \eta S \\ \dot{E}(t) = \beta_u SU + \beta_v SV - \nu_1 E - a_1^* \nu_2 E \\ \dot{U}(t) = \nu_1 E - d_1 U - \xi U \\ \dot{V}(t) = a_1^* \nu_2 E - \alpha V - d_2 V \\ \dot{H}(t) = \alpha V - d_3 H - a_2^* \gamma H \\ \dot{R}(t) = \xi U + a_2^* \gamma H + \eta S - \delta R \end{cases} \quad (11)$$

with initial conditions

$$\begin{cases} S(0) = S_0, \quad E(0) = E_0, \quad U(0) = U_0, \\ V(0) = V_0, \quad H(0) = H_0, \quad R(0) = R_0 \end{cases} \quad (12)$$

$$\begin{cases} \dot{p}_1 = S - S^* + (\beta_3 U + \beta_4 V)(p_2 - p_1) + \eta(p_6 - p_1) \\ \dot{p}_2 = E + \nu_1(p_3 - p_2) + a_1^* \nu_2(p_4 - p_2) \\ \dot{p}_3 = U + \beta_3 S(p_2 - p_1) + \xi(p_6 - p_3) - d_1 p_3 \\ \dot{p}_4 = V + \beta_4 S(p_2 - p_1) + \alpha(p_5 - p_4) - d_2 p_4 \\ \dot{p}_5 = H + a_2^* \gamma(p_6 - p_5) - d_3 p_5 \\ \dot{p}_6 = R - R^* + \delta(p_1 - p_6) \end{cases} \quad (13)$$

with transversality conditions

$$p_i(T) = 0, for\ all\ i \in \Lambda \quad (14)$$

Furthermore a^* is characterized by

$$a^*(t) = \left[\max(0; \min(a_1^*(t); 1); \max\left(0; \min(a_2^*(t); 1)\right)\right] \quad (15)$$

with

$$a_1^*(t) = \frac{\nu_2 E(t)(p_E(t) - p_V(t))}{\varepsilon_1},$$

and

$$a_2^*(t) = \frac{\gamma H(t)(p_H(t) - p_R(t))}{\varepsilon_2}.$$

***Proof*:** From the Pontryagin's Maximum Principle, if (a^*, X^*) is optimal then we have the following Hamiltonian systems:

$$\dot{X}_i = \frac{\partial \mathcal{H}}{\partial p_i} \quad \text{for } i \in \Lambda \quad \text{with } \mathrm{X}_i(0) = \mathrm{X}_{i0} \tag{16}$$

$$\dot{p}_i = -\frac{\partial \mathcal{H}}{\partial \boldsymbol{X_i}} \quad \text{for } i \in \Lambda \quad \text{with } p_i(T) = 0 \tag{17}$$

and

$\mathcal{H}(a^*) = \min_{a \in [0;1]^2} \mathcal{H}(a)$.

If $a^* \in]0;1[^2$ then

$\frac{\partial \mathcal{H}}{\partial a} = 0$.

Solving this equation yields

$a_1^*(t) = \frac{\nu_2 E(t)\left(p_E(t) - p_V(t)\right)}{\varepsilon_1}$,

and

$a_2^*(t) = \frac{\gamma H(t)\left(p_H(t) - p_R(t)\right)}{\varepsilon_2}$.

Since $a^* \in [0;1]^2$ then Equation (15) is deduced. Calculating Equations (16) and (17) gives Equations (11) and (13).

4.2 Dynamic Programming Principle

The optimal control problems (7)-(4) can be solved by solving a first order partial differential equation called Hamilton-Jacobi equation.

Let $Z(t, \mathbf{X}_t)$, known as the value function, be the value of the objective function J from t to T when an optimal policy is followed from t to T, given $\mathbf{X}_t = \mathbf{x}$:

$Z(t, \mathbf{x}) = \min_{a \in \mathcal{A}} J(t, \mathbf{x}, a)$,

with $J(t, \mathbf{x}, a) = \frac{1}{2}\int_t^T L\,(s, \mathbf{X}_s, a)\, ds$.

Now, we are going to give the Hamilton-Jacobi equation by using dynamic programming principle.

Theorem 6. *Suppose that $Z \in \mathcal{C}^1([0;T] \times \Omega)$, then the following dynamic programming equation:*

$$\begin{cases} -\frac{\partial Z}{\partial t} + H(t, x, DZ) = 0 \ \ in\ [0;T] \times \Omega \\ \qquad\qquad Z(\mathbf{x}, T) = 0 \ \ on\ \Omega, \end{cases} \tag{18}$$

holds.

With for $(t, x, p) \in [0;T] \times \Omega \times \mathbb{R}^6$

$H(t, x, p) = \sup_{a \in \mathcal{A}} [-L(t, x, a) - p \cdot f] = \sup_{a \in \mathcal{A}} [-\mathcal{H}(t, x, p, a)]$.

Before doing the proof, let's give the following dynamic programming principle.

Lemma 1. *For any initial condition* $(t,x) \in [0;T] \times \bar{\Omega}$,

$$Z(t,x) = \inf_{a\in\mathcal{A}} \left[\int_t^{t+h} L\left(s,x(s),a(s)\right)ds + Z\left(t+h,x(t+h)\right)\right] \quad (19)$$

***Proof*:** Of theorem 6, By dynamic programming principle (19) in lemma 1, we have for small $h > 0$ for any $a \in \mathcal{A}$,

$$\begin{aligned} Z(t,x) \leq & \int_t^{t+h} L\left(s,x(s),a(s)\right)ds + Z\left(t+h,x(t+h)\right) \\ 0 \leq & \int_t^{t+h} L\left(s,x(s),a(s)\right)ds + Z\left(t+h,x(t+h)\right) - Z(t,x) \\ 0 \leq & \frac{1}{h}\int_t^{t+h} L\left(s,x(s),a(s)\right)ds + \frac{1}{h}\left[Z\left(t+h,x(t+h)\right) - Z(t,x)\right] \end{aligned}$$

Then passing to the limit $h \to 0$ yields

$$0 \leq L\left(t,x(t),a(t)\right) + \frac{\partial Z}{\partial t}(t,x) + f(t,x,a)\cdot D_x Z\ .$$

Finally, multiplying by (-1) and taking the sup yield

$$-\frac{\partial Z}{\partial t} + H(t,x,DZ) \leq 0.$$

Assuming a^* is the optimal control and x^* the corresponding optimal trajectory. Moreover, since Z is C^1 and $\mathcal{A}$ is compact then by the dynamic programming principle we have

$$Z(t,x^*) = \int_t^{t+h} L(s,x^*,a^*)ds + Z\left(t+h,x^*(t+h)\right).$$

Using the same arguments and steps as above:

$$-\frac{\partial Z}{\partial t} + H(t,x,DZ) = 0.$$

5. Numerical Simulations

In this section, the aim is to illustrate the results obtained by numerical simulations based on real data from COVID-19 in Senegal. This involves analyzing the impact of the controls on the evolution of the disease. To do this, we make a comparison between the ODE and the OCP based on three tests:

- **Test 1:** low vaccination rate $\eta = 0.00127269$, lower re-susceptibility rate $\delta = 6.36347\ 10^{-6}$ and high hospitalization rate $\alpha = 0.7$.
- **Test 2:** high vaccination rate $\eta = 0.0127269$, low re-susceptibility rate $\delta = 6.36347\ 10^{-4}$ and low hospitalization rate $\alpha = 0.07$.
- **Test 3:** high vaccination rate $\eta = 0.0127269$, high re-susceptibility rate $\delta = 6.36347\ 10^{-2}$ and low hospitalization rate $\alpha = 0.07$.

The tests come from the paper (Ly et al., 2022). The authors fitted the parameters of the tests to Senegal's Covid-19 data.

The initial population is set to $8 \cdot 10^6$ and the initial states to: $S_0 = 785.7353 \cdot 10^3$, $E_0 = 150.42 \cdot 10^3$, $U_0 = 1.2043 \cdot 10^3$, $V_0 = 7.4412 \cdot 10^3$, $H_0 = 4.8786 \cdot 10^3$, $R_0 = 1.9154 \cdot 10^3$.

We use Gekko Optimization Suite (Beal et al., 2018) in python (Van Rossum, 1995). We use the same real data as in the paper (Ly et al., 2022). We make simulations of 365 days.

The following **Table 2** gives the parameters for the three tests we performed:

Table 2. Table of parameters: values of parameters for different tests.

Parameters	Values of test 1	Values of test 2	Values of test 3
δ	$6.36347 \cdot 10^{-6}$	$6.36347 \cdot 10^{-4}$	$6.36347 \cdot 10^{-2}$
β_u	$2.65884 \cdot 10^{-8}$	$2.65884 \cdot 10^{-8}$	$2.65884 \cdot 10^{-8}$
β_v	$2.53223 \cdot 10^{-8}$	$2.53223 \cdot 10^{-8}$	$2.53223 \cdot 10^{-8}$
η	0.00127269	0.0127269	0.0127269
v_1	0.141481	0.141481	0.141481
v_2	0.141481	0.141481	0.141481
d_1	0.001	0.001	0.001
d_2	0.001	0.001	0.001
d_3	0.001	0.001	0.001
ξ	0.05	0.05	0.05
α	0.7	0.07	0.07
γ	0.0667	0.0667	0.0667

The necessary controls to reduce the pandemic in different situations or tests will be analyzed. The tests will show that the effort needed to control and reduce the disease may depend on vaccination, re-susceptibility, and hospitalization rate.

5.1 Case Study: ODE

In this subsection, numerical simulations of the ODE model (1) are given to see the evolution of the disease without applying any strategy. That is, there is no control in the model (**Figure 2**).

5.2 Case Study: OCP

Numerical results of the optimal control problem are shown in this subsection. **Figures 3** and **4** describe respectively optimal states and optimal controls and objective function of test 1.

Figures 5 and **6** show respectively optimal states and controls and objective function of test 2.

Figures 7 and **8** refer respectively optimal states and optimal controls and objective function of test 3.

Figure 9 compares the optimal control infected states with EDO infected states.

Figure 10, for each state, gives a comparison between the result of test 1, test 2, and test 3.

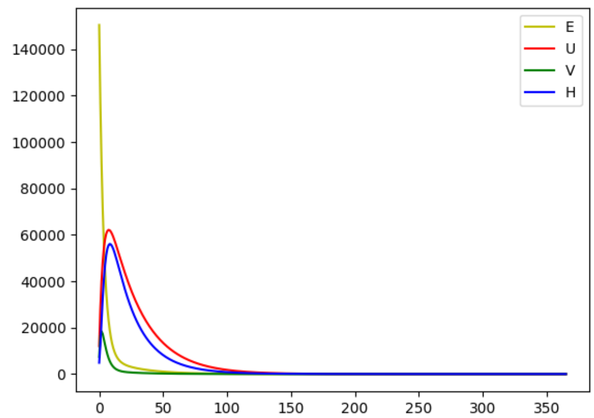

States E, U, V, H.

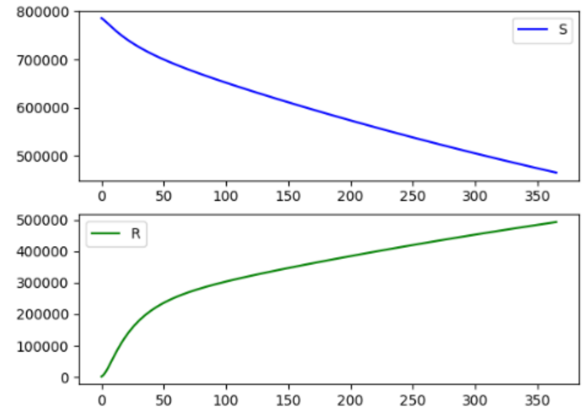

States S, R.

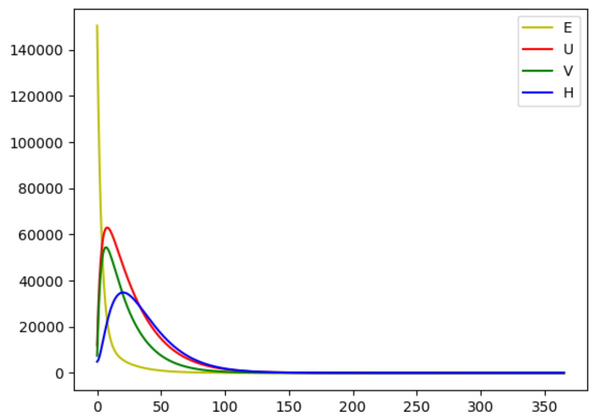

States E, U, V, H.

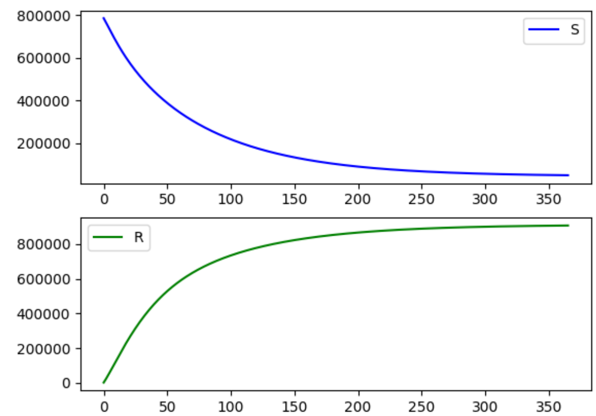

States S, R.

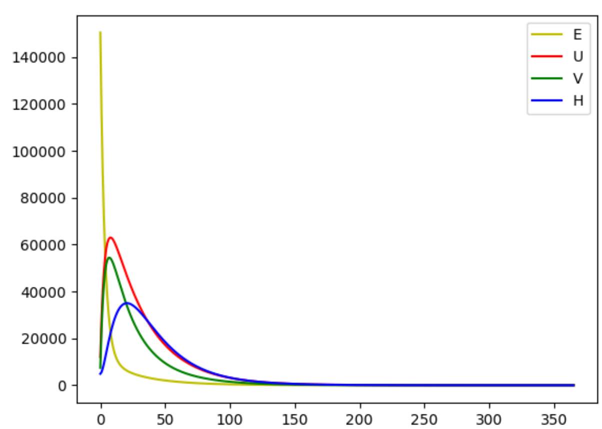

States E, U, V, H.

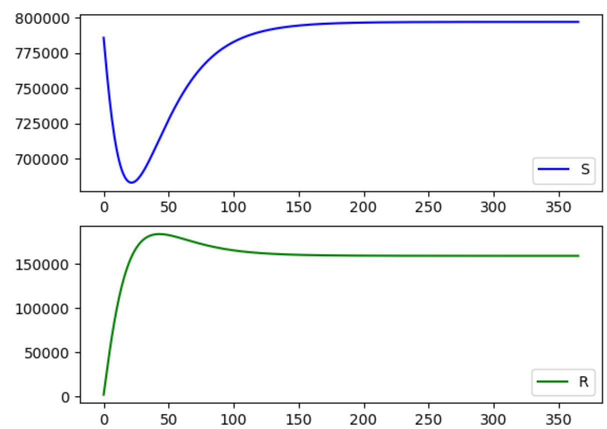

States S, R.

Figure 2. Tests: States Exposed(E), Unknown cases(U), Known cases (V), and Hospitalized (H) in the left and States Susceptible(S), Recovered(R) in the right.

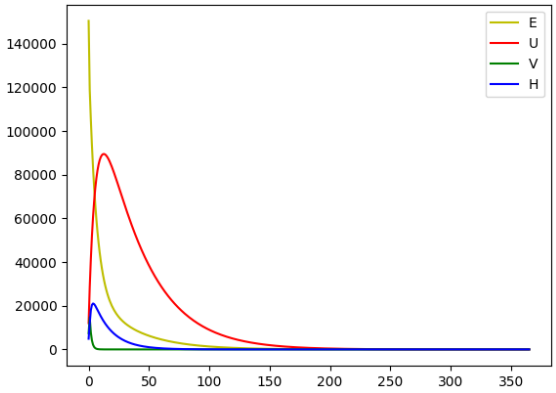

Optimal states E, U, V, H.

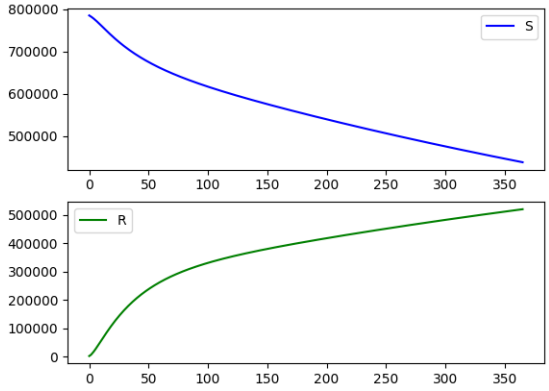

Optimal states S, R.

Figure 3. Test 1: optimal states.

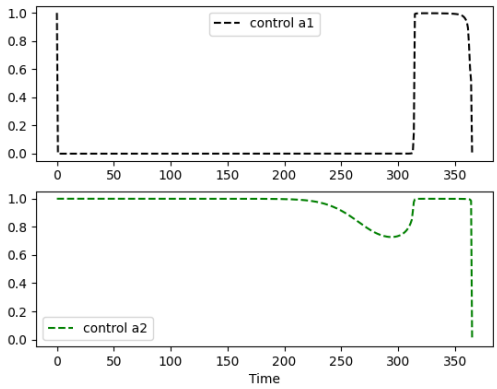

Optimal controls.

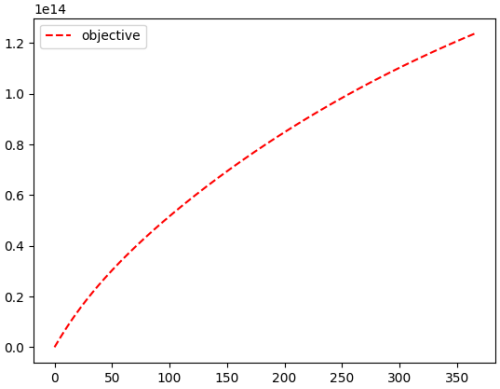

Objective.

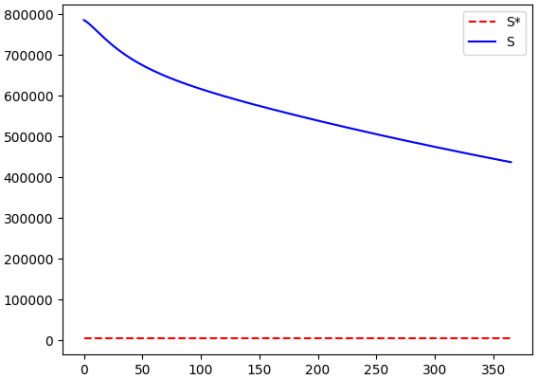

Optimal states S and equilibrium S*.

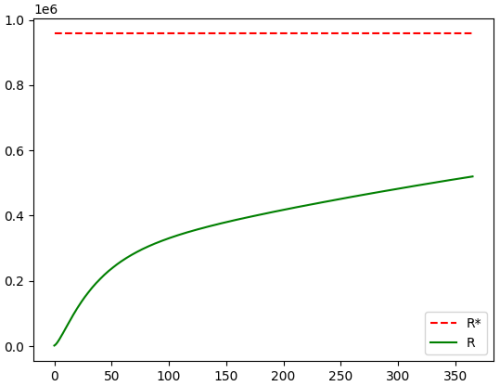

Optimal states R and equilibrium R*.

Figure 4. Test 1: Controls, objective function and S, R states and equilibrium.

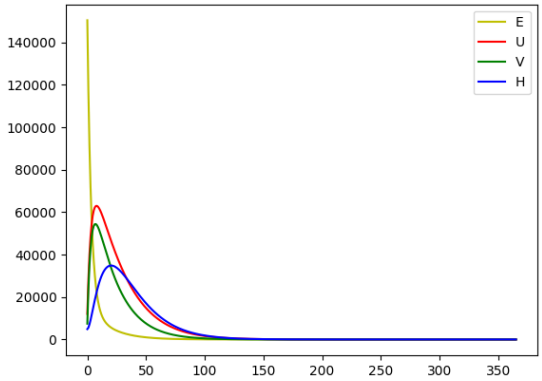

Optimal states E, U, V, H.

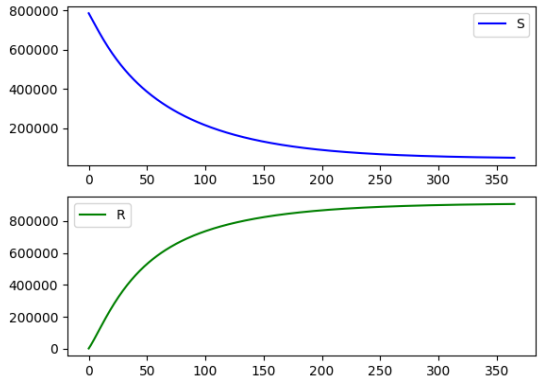

Optimal states S, R.

Figure 5. Test 2: optimal states.

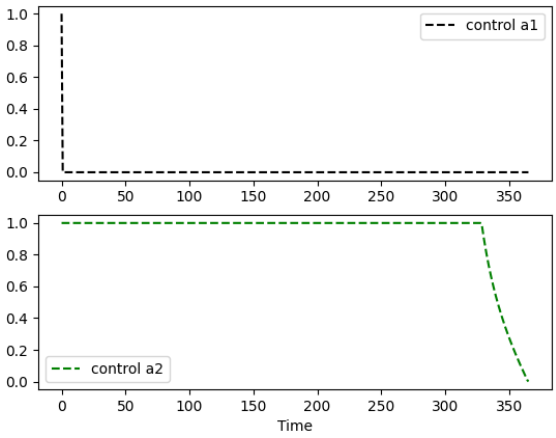

Optimal controls.

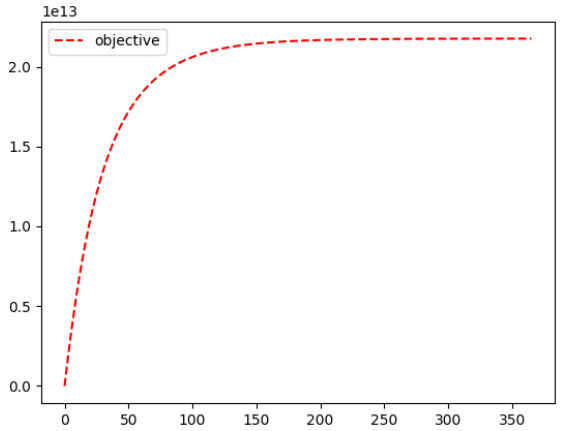

Objective.

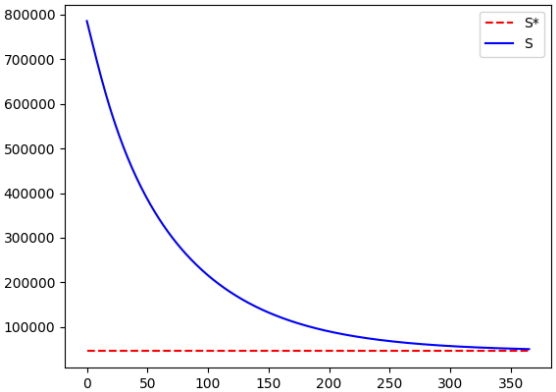

Optimal states S and equilibrium S*.

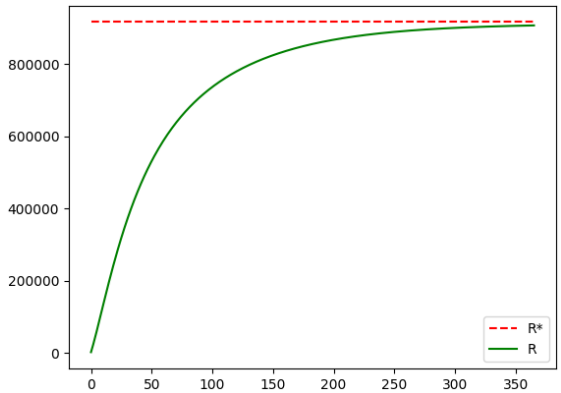

Optimal states R and equilibrium R*.

Figure 6. Test 2: Controls, objective function and S, R states and equilibrium.

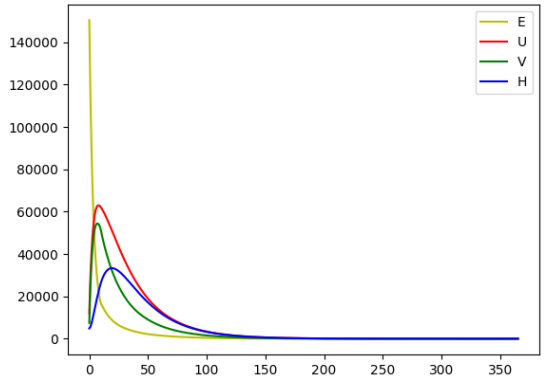

Optimal states E, U, V, H.

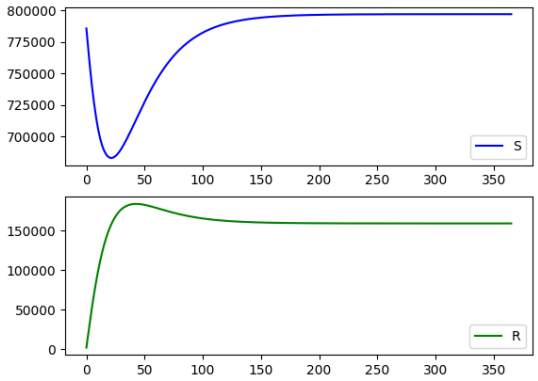

Optimal states S, R.

Figure 7. Test 3: optimal states.

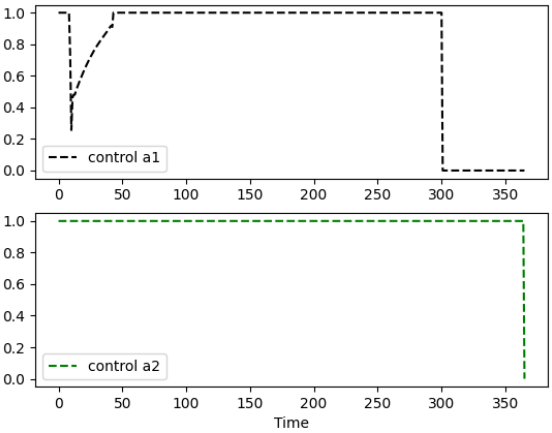

Optimal controls.

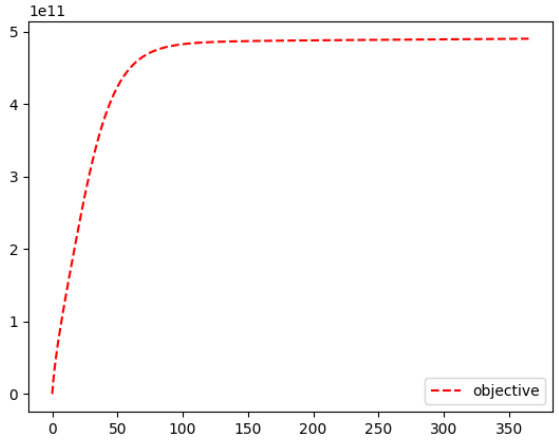

Objective.

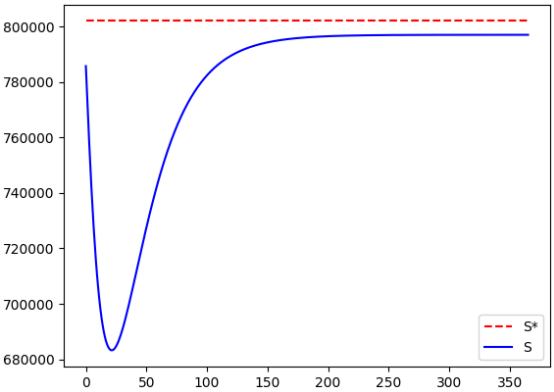

Optimal states S and equilibrium S*.

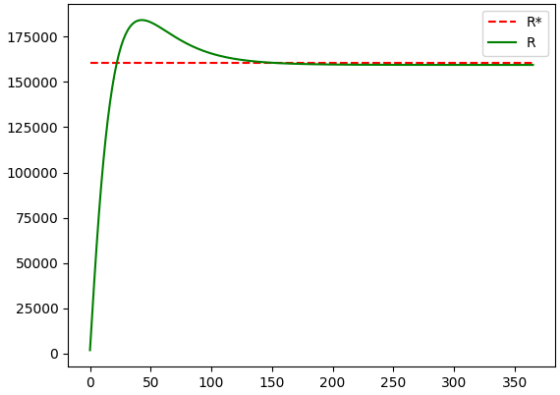

Optimal states R and equilibrium R*.

Figure 8. Test 3: Controls, objective function and S, R states and equilibrium.

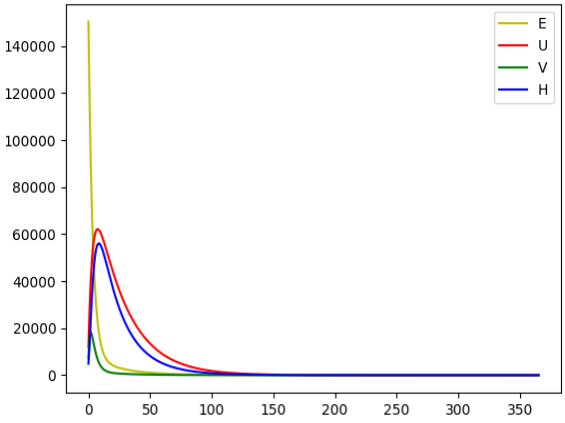

Test 1: Without controls.

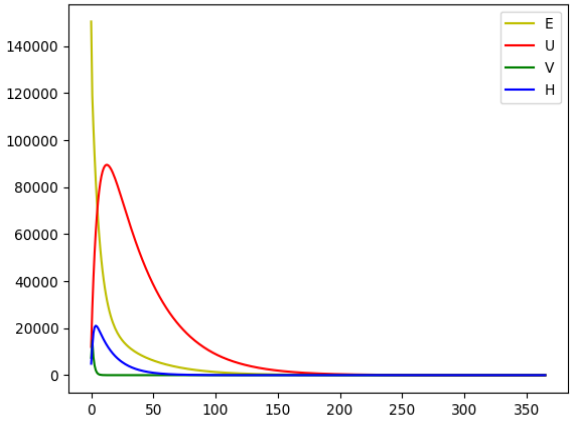

Test 1: Controlled.

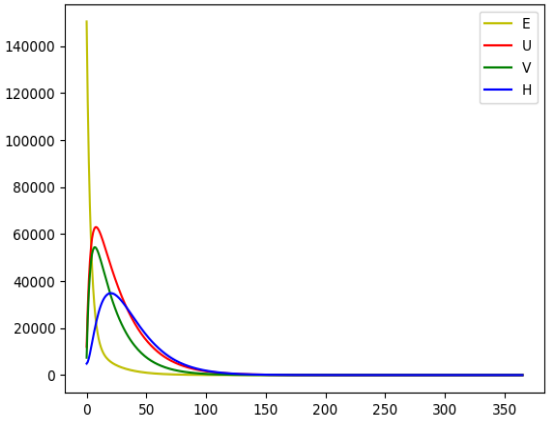

Test 2: Without controls.

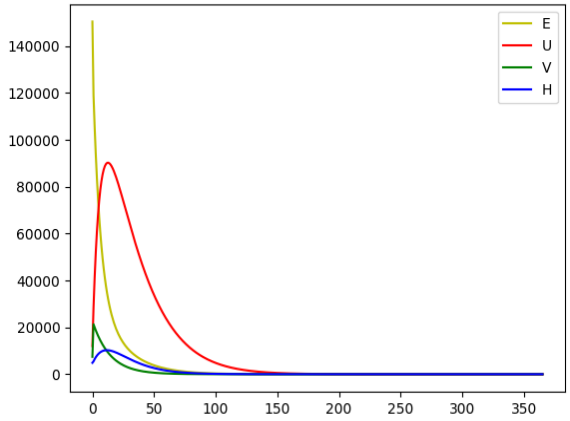

Test 2: Controlled.

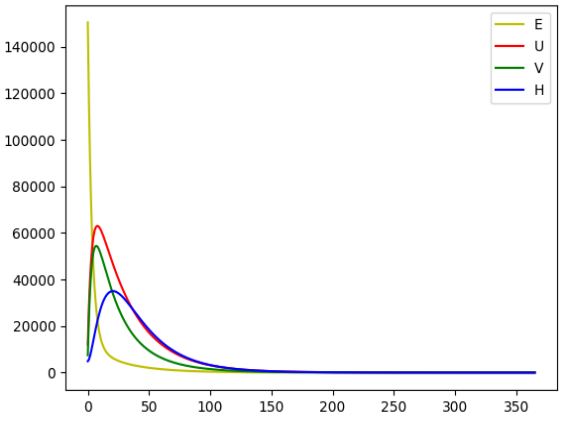

Test 3: Without controls.

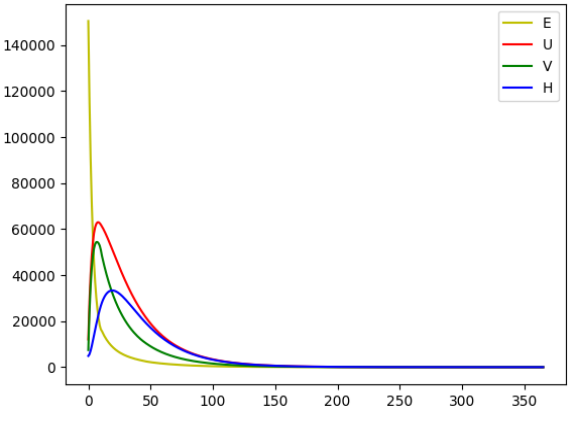

Test 3: Controlled.

Figure 9. Tests: States without control in the left and controlled States in the right, test 1, test 2 and test 3.

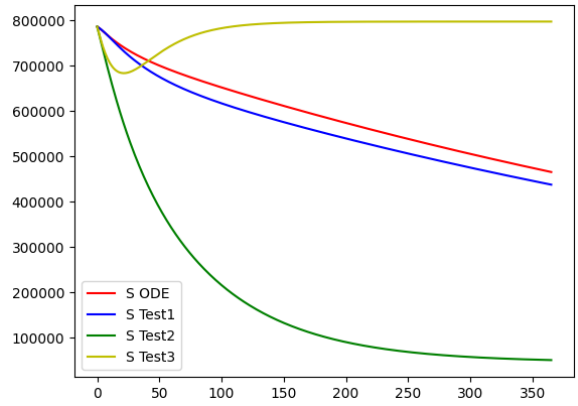

Susceptible.

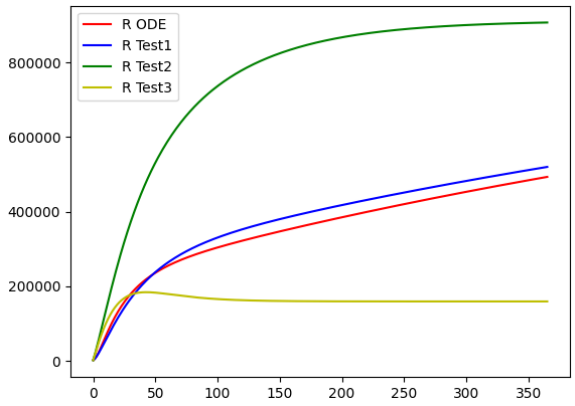

Recovered.

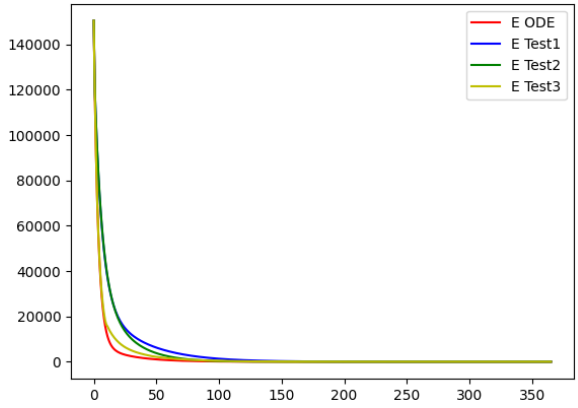

Exposed.

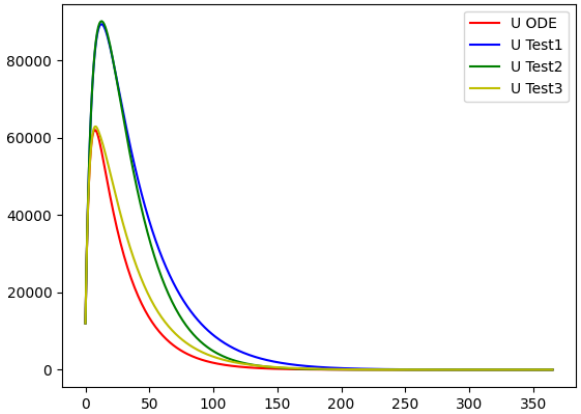

Unconfirmed.

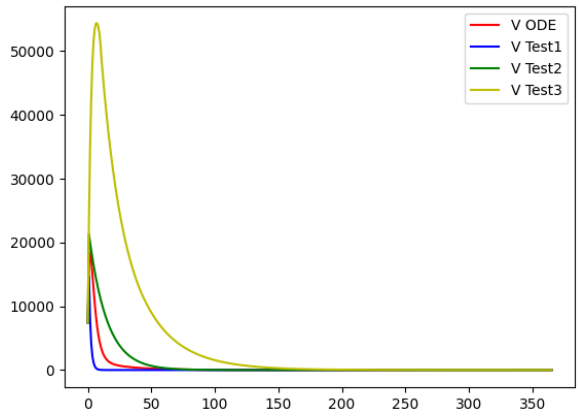

Confirmed.

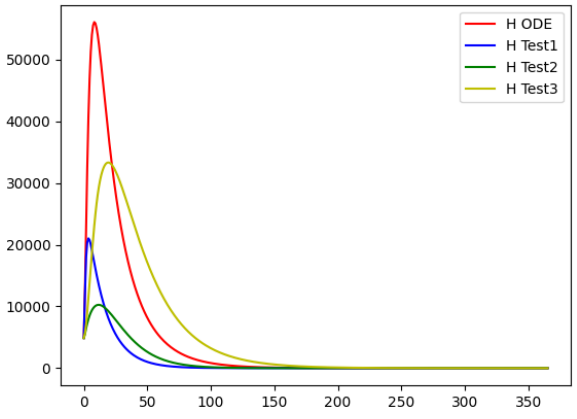

Hospitalized.

Figure 10. Comparative plot of States. Without control, test 1, test 2, test 3, for each state.

5.3 Discussion

Through the figures, the following two situations are compared:

- No strategy is implemented to optimize the detection of the disease and treatment. It is the situation 'Without Control'.
- Strategies on detection campaigns and patient treatments are applied in order to stem the disease as quickly as possible. It is the situation 'controlled' or 'with control'.

For the test 1 'without controls', the number of hospitalizations increases considerably until reaching a peak of almost 60000 on the 10th day, then decreases and converges towards zero from the 100th day. We see the same trend with the test 1 'controlled' case except that the peak is reached after 5 days and is about 20000. The convergence of H to zero is faster after 50 days. For the unconfirmed cases, the highest peak and the slowest convergence are obtained in the case 'with controls'. The exposed individuals are slower with the controlled system than the uncontrolled one. On the other hand, the evolution of confirmed is faster in the 'controlled' case than in 'without controls'. All these results can be explained by the fact that during the first 150 days, the detection campaign is nil, and the treatment is maximal during the first 75 days (see **Figure 4**: optimal controls). By noting that the number of susceptible begins and the number of recovered increases, the proposed treatment is reduced from the 75th day to the 150th day. Between the 150th and the 200th, the emphasis is on the detection campaign, which is maximal, and the proposed treatment increases.

Figure 6 'Test 2: optimal controls' shows that treatment is at the maximum, which lowers the number of hospitalized in 'Test 2: controlled' of **Figure 9** compared to 'Test 2: without controls'. E, H, and V converge very fast to their equilibrium values with the 'controlled' model. Only the trajectory of U is slow to converge towards zero because the detection is zero during the 200 days in **Figure 9** 'Test 2: controlled'; therefore, the unknown cases increase, which delays the convergence towards the value at equilibrium. Figures 6 'Optimal states S and equilibrium S*' and 'Optimal states R and equilibrium R*' show that S and R converge respectively to S^* and R^*.

Figure 9 'Test 3: without controls' and 'Test 3: controlled' show that the trajectories of the two systems are quite similar. We notice that the trajectories of E, U, V, and H converge slightly faster with a 'controlled' system. **Figure 8** 'Optimal states S and equilibrium S*' and 'Optimal states R and equilibrium R*' give the trajectories of S and R. The vaccination is high in this test. Therefore, during the first 25 days, the number of susceptible S decreases while the number of cured increases R due to the decrease in S and the fact that the treatment is at the maximum in **Figure 8** 'optimal controls'. From the 25th day, the number of healed has reached its maximum, so many of them become susceptible again because of the high rate of re-susceptibility, which explains the decrease in R and the increase in S. Also, we note a convergence of S towards S^* and of R towards R^*.

Senegal COVID-19 data is biased, heterogeneous and incomplete. The model parameters are calibrated on this data to make simulations, and their imperfection will affect the results obtained. Even though the data are imperfect, whatever the country, results can provide useful information that can help decision-making. To better take into account imperfections in data, a consideration of delays in the model as in (Ng and Gui, 2020) or / and a use of stochastic model as in (Ly et al., 2020) could be more suitable. However, unlike (Ng et al., 2020), the repetitive wave effect is prevented thanks to vaccination on the one hand and controls of detection and care provided to patients. In addition, in (Ly et al., 2022), the controls obtained are "bang-bang" type, which are generally difficult to implement in practice. On the contrary in our work because of the deterministic nature of the model studied, we have obtained regular controls easier to implement in practice.

6. Conclusion

In this work, we were interested in an optimal control problem of a deterministic model of transmission of COVID-19. The idea is to move the system towards disease-free equilibrium by minimizing a functional centered at the DFE. We have proved the existence of optimal control and trajectories and solved the problem using the Pontryagin maximum principle and the dynamical programming principle. Numerical simulations show that exercising controls on the detection campaign and treatment brings the system back to an equilibrium state, making it possible to control the disease evolution.

The results have shown the effectiveness of setting up controls on detection campaigns and patient treatments. Indeed, these optimized controls made it possible to reduce the accumulation of confirmed cases and thus stem the disease faster. The possibility that individuals healed can contract the disease again is a very serious problem. Indeed, this leads to a wave effect of the disease, that is to say, that it comes back periodically. Vaccination and controls applied to detection and treatment made it possible to reduce the evolution of the disease.

As a perspective on this work, fractional Brownian motion can be introduced to our model and optimal control theory applied. More data can be exploited, and Deep learning can be used to estimate parameters and make sensibility analyses.

Conflict of Interest

The authors confirm that there is no conflict of interest to declare for this publication.

AI Disclosure

The authors declare that no assistance is taken from generative AI to write this article.

Acknowledgments

This research did not receive any specific grant from funding agencies in the public, commercial, or not-for-profit sectors. The authors would like to thank the editor and anonymous reviewers for their comments that help improve the quality of this work.

References

Ahmed, I., Modu, G.U., Yusuf, A., Kumam, P., & Yusuf, I. (2021). A mathematical model of coronavirus disease (COVID-19) containing asymptomatic and symptomatic classes. *Results in Physics, 21*, 103776.

Baldé, M.A.M.T. (2020). Fitting SIR model to COVID-19 pandemic data and comparative forecasting with machine learning. *MedRxiv Preprint*, 1-20. https://doi.org/10.1101/2020.04.26.20081042.

Baldé, M.A.M.T., Baldé, C., & Ndiaye, B.M. (2020). Impact studies of nationwide measures COVID-19 anti-pandemic: compartmental model and machine learning. *Communications in Mathematical Biology and Neuroscience.* arXiv:2005.08395. https://doi.org/10.48550/arxiv.2005.08395.

Beal, L.D.R., Hill, D.C., Martin, R.A., & Hedengren, J.D. (2018). GEKKO optimization suite. *Processes*, *6*(8), 106. https://doi.org/10.3390/pr6080106.

Firmansyah, F., & Rangkuti, Y. (2023). Sensitivity analysis and optimal control of COVID-19 model. *Jambura Journal of Biomathematics*, *4*(1), 95-102. http://dx.doi.org/10.34312/jjbm.v4i1.19025.

Fleming, W.H., & Rishel, R.W. (1975). *Deterministic and stochastic optimal control*. Springer-Verlag, Berlin, Heidelberg, New York. ISBN: 978-1-4612-6382-1(p), 978-1-4612-6380-7(e).

Kamgang, J.C., & Sallet, G. (2008). Computation of threshold conditions for epidemiological models and global stability of the disease-free equilibrium (DFE). *Mathematical Biosciences, 213*(1), 1-12. https://doi.org/10.1016/j.mbs.2008.02.005.

Kifle, Z.S., & Obsu, L.L. (2023). Optimal control analysis of a COVID-19 model. *Applied Mathematics in Science and Engineering, 31*(1), 2173188. https://doi.org/10.1080/27690911.2023.2173188.

Ly, S., Tendeng, L., Balde, M.A.M.T., Ngom, D., & Seck, D. (2022). Stochastic reaction network modeling and optimal control for Covid-19. In: Seck, D., Kangni, K., Nang, P., Sambou, M.S. (eds) *Nonlinear Analysis, Geometry and Applications. Trends in Mathematics.* Birkhäuser, Cham, pp. 121-141. https://doi.org/10.1007/978-3-031-04616-2_5.

Mansal, F., Baldé, M.A.M.T., & Bah, A.O. (2024). Optimal control on a mathematical model of SIR and application to Covid-19. In: Seck, D., Kangni, K., Sambou, M.S., Nang, P., Fall, M.M. (eds) *Nonlinear Analysis, Geometry and Applications. Trends in Mathematics* (pp. 101-128). Birkhäuser, Cham. https://doi.org/10.1007/978-3-031-52681-7_4.

Ndiaye, B.M., Tendeng, L., & Seck, D. (2020a). Analysis of the COVID-19 pandemic by SIR model and machine learning technics for forecasting. https://arxiv.org/pdf/2004.01574.pdf.

Ndiaye, B.M., Tendeng, L., & Seck, D. (2020b). Comparative prediction of confirmed cases with COVID-19 pandemic by machine learning, deterministic and stochastic SIR models. https://arxiv.org/pdf/2004.13489.pdf.

Ng, K.Y., & Gui, M.M. (2020). COVID-19: Development of a robust mathematical model and simulation package with consideration for ageing population and time delay for control action and resusceptibility. *Physica D: Nonlinear Phenomena, 411,* 132599. https://doi.org/10.1016/j.physd.2020.132599.

Teschl, G. (2012). *Ordinary differential equations and dynamical systems*. American Mathematical Society, ISBN 978-0-8218-8328-0.

Van den Driessche, P., & Watmough, J. (2002). Reproduction numbers and sub-threshold endemic equilibria for compartmental models of disease transmission. *Mathematical Biosciences, 180*(1-2), 29-48. https://doi.org/10.1016/S0025-5564(02)00108-6.

Van Rossum, G. (1995). *Python tutorial*. Centrum voor Wiskunde en Informatica, Amsterdam, The Netherlands.

Wang, L., Zhang, Q., & Liu, J. (2022). On the dynamical model for COVID-19 with vaccination and time-delay effects: a model analysis supported by Yangzhou epidemic in 2021. *Applied Mathematics Letters, 125*, 107783. https://doi.org/10.1016/j.aml.2021.107783.